Hindawi
Advances in Civil Engineering
Volume 2024, Article ID 3870669, 15 pages
https://doi.org/10.1155/2024/3870669

Research Article

Vehicle–Bridge Interaction Dynamic Analysis of Continuous Rigid Frame Composite Box Girder Bridge with Corrugated Steel Webs under Seismic Excitation

Peng Qiao, Chen Ma, Chang-Jiang Duan, Hao Lei, Heng Zhao, and Jun He

School of Civil Engineering, Chang'an University, Xi'an 710061, Shaanxi, China

Correspondence should be addressed to Jun He; hejun@chd.edu.cn

Received 28 August 2023; Revised 6 December 2023; Accepted 27 January 2024; Published 23 February 2024

Academic Editor: Meng Gao

To study the vehicle–bridge interaction (VBI) of highway bridges under seismic excitation, a vehicle–bridge couple analysis method based on Ansys is proposed. The 1/2 vehicle model and space beam element model were established to analyze the VBI response of Lanzhou Xiaoshagou bridge. The self-excited excitation of the system is represented by road surface irregularity randomness, while the external excitation is represented by an earthquake. The impact of seismic types, seismic direction, seismic intensity, vehicle speed, and road surface irregularity on the bridge vibration under the vehicle–bridge coupling during an earthquake is thoroughly analyzed. The results reveal that the type of earthquake significantly influences the dynamic response of the bridge, showing a minimum difference of 31.4%. The intensity of the earthquake is positively correlated with the dynamic response of the bridge. Longitudinal and vertical earthquakes have a more noticeable effect on the bridge's vertical vibration compared to lateral earthquakes. The ratio of the bridge response under vertical or longitudinal seismic excitation to the response of lateral earthquakes ranges from 1.50 to 26.61. Vehicle speed, road irregularity grade, and randomness have a negligible impact on the dynamic response of vehicle–bridge interaction under an earthquake, accounting for less than 3%. These findings indicate that the analysis of earthquake-bridge vibration can simplify the VBI analysis for continuous rigid frame composite box girder bridges with corrugated steel webs under seismic conditions.

1. Introduction

The composite box girder bridges with corrugated steel webs, originated in France, have been widely used in bridge engineering in Japan and China due to its advantages such as lightweight and superior load-bearing performance compared to ordinary prestressed concrete bridges. Among the various composite box girder bridge with corrugated steel webs, the continuous rigid frame box girder bridge with corrugated steel web, which has the advantages of small deformation, high stiffness, comfortable driving experience, and ease of construction, has been constructed more in China. By the end of 2022, there were already more than 21 built and under-construction continuous rigid frame box girder bridges with corrugated steel webs in China.

China is a country prone to frequent earthquakes. On one hand, as the span of these bridges continues to increase, it increases the possibility of seismic-vehicle-bridge coupled vibration. On the other hand, although scholars have conducted relatively systematic research on the vehicle–bridge coupled vibration of concrete box girder railway bridges under seismic excitation, compared to concrete box girder bridges, this type of bridge can significantly reduce seismic forces. When this type of bridge is subjected to vehicle–bridge coupled and seismic coupled interaction, the sensitivity of various factors to the dynamic response of the vehicle–bridge coupled interaction may differ from that of concrete bridges. Therefore, it is necessary to study the vehicle–bridge coupled vibration of highway bridges under seismic excitation and clarify the relevant laws of seismic-vehicle-bridge coupled vibration caused by various factors. However, few studies have been done on the vehicle–bridge coupled vibration of highway bridges under seismic excitation so far, especially regarding composite box girder bridge with corrugated steel webs [1, 2].

At present, the seismic-vehicle-bridge coupling has been widely studied in the field of railway bridges, mainly focusing on the response of vehicles and bridges under seismic excitation, as well as issues related to vehicle safety. Zhongxian et al. [3] analyzed the light rail railroad and compared the vibration of the Tianjin wave and El Centro wave on the vehicle–bridge coupled system. It was concluded that the seismic-vehicle-bridge coupling interaction satisfies the superposition principle, and the coupling effect can be approximated as the sum of the bridge's vibration response under seismic loads and the vehicle–bridge coupled dynamic response. Zhihui et al. [4] and Hujun et al. [5] conducted a comparative analysis of the dynamic response of bridges and trains under different train speeds and seismic intensities and provided threshold values for the safe operation of trains under various levels of seismic motion. Du et al. [6] compared and analyzed the effects of seismic motion displacement and acceleration input modes on the seismic-vehicle–bridge coupling dynamic response. Hujun and Xiaozhen [7] further compared commonly used nonuniform analysis methods in seismic-vehicle–bridge coupling analysis, which are direct solution method, relative motion method, large mass method, and large stiffness method. Zhi et al. [8] compared and analyzed the influence of seismic spectrum characteristics on the dynamic response of bridges. Ziming et al. [9] based on the principle of minimum potential energy and with the seismic-vehicle-bridge coupling, compared the dynamic response of the horizontal and vertical seismic waves on the railroad bridge. In summary, the current research mainly focuses on vibration analysis of railway bridges under seismic excitation, while research on seismic-vehicle-bridge coupling vibration in highway bridges is scarce.

In terms of research methods for vehicle–bridge coupled vibration, the current methods mainly include development methods for vehicle–bridge coupled interaction based on Fortran language, combined simulation methods using multibody software and finite element software, and combined simulation methods based on MATLAB and Ansys finite element. The current Ansys vehicle–bridge coupled method based on secondary development. Chengzhao [10], Wang et al. [11], and Li et al. [12] established the bridge model by Ansys preprocessing function, introduced two conditions of geometric compatibility of vehicle and bridge and the opposite direction of the vehicle–bridge coupled forces by using Fortran language, and realized the vehicle–bridge coupling based on Newmark-β stepwise integration method. Jianrong [13] adopts the method of combining Ansys with the self-programmed VBDIP (Vehicle Bridge Dynamic Interaction Program); Jianrong [14] adopts the method of combining Ansys and UM software; Peiwen et al. [15] and Shizhong [16] propose the method of implementing vehicle–bridge coupling in a single Ansys environment; however, the proposed methods are subject to the secondary development of Ansys language, which is difficult to implement for the general researchers. To address this problem, this paper proposes a contact constraint-based vibration analysis method for axle coupling, which can better realize the simulation of road surface irregularity [17] and simplify the analysis method of vehicle–bridge coupled interaction. Jin et al. [18] based on a numerical model of a train-track-bridge system with 31° of freedom showed that vertical seismic excitation promotes wheel bulging and increases the chance of derailment. In addition, the risk of derailment generally increases with the ratio of lateral to vertical deck acceleration. Paraskeva et al. [19] investigated the seismic response of a vehicle–bridge interaction (VBI) system under vertical seismic excitation, modeling a truck vehicle as a rigid body assembly. A parametric study is carried out based on a realistic highway (straight R/C) bridge–truck case. The analysis presents two main sources of dynamic excitation which is an inherently unpredictable "vehicle-bridge-seismic time" problem requiring probabilistic treatment. Zhou et al. [20] established the equations of motion of the monorail train and solved them by self-programming on the MATLAB platform. A finite element model of the bridge was developed and solved using Ansys programing method. The bridge and vehicle subsystems are coupled by global iteration with the exchange of wheel–rail contact forces. The cosimulation method is validated by the dynamic response of the monorail train and the bridge reported in the related literature. Su et al. [21] proposes a method for evaluating the fatigue life of tied-arch bridge suspenders by considering the effects of random cyclic traffic loads and environmental erosion. Yu et al. [22] in order to cover the complexity of coding and extend the generality on the road vehicle–bridge iteration, a process to solve VBI considering varied vehicle speed based on a convenient combination of MATLAB Simulink and Ansys is presented. Zou et al. [23] cover the effects of different VBI models on the bridge responses are studied and the results from different models are compared in terms of their accuracy, efficiency, and suitability.

Compared to railway bridges, highway bridges have smaller live loads, and the vibration characteristics caused by vehicles may differ from those of trains. Moreover, the seismic performance of composite box girder bridge with corrugated steel webs is better than that of railway bridges. Therefore, whether the seismic-vehicle-bridge coupling laws of railway bridges can be directly applied to highway bridges requires further research. In this regard, this paper proposes a contact–constraint-based vehicle–bridge coupling vibration analysis method. Subsequently, taking the Xiaoshagou Bridge as a case study, a 1/2 vehicle model is established, and the contact–constraint-based vehicle–bridge coupling vibration analysis method is used to investigate the influence of seismic motion types, directions, and intensities on the vertical dynamic response of seismic-vehicle-bridge coupling. Then, the correlation between the vertical dynamic response of the bridge is summarized and the influence of factors such as vehicle speed, road surface irregularity level, and randomness of road surface irregularity is analyzed under seismic excitation coupling. Finally, a comparison is made between the vehicle–bridge coupling vibration and the dynamic response of the bridge under seismic action, to show the simplified analysis of seismic-vehicle-bridge coupling vibration in highway bridges.

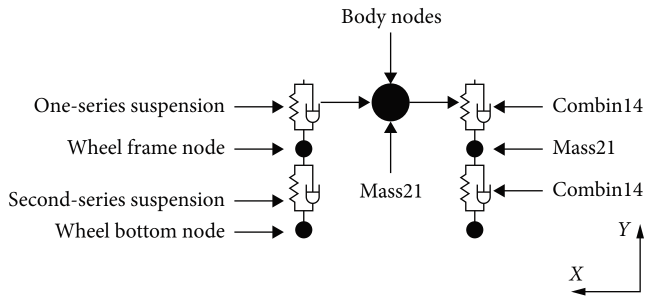

FIGURE 1: Modern vehicle model and element equivalence: 1/2 vehicle model and equivalent.

TABLE 1: Unit selection and setting of vehicle model components in Ansys.

Vehicle component categories	Ansys element simulation	Element option settings
Car body	Mass21	Keyopt (3) = 4
Suspension system	Combin14	Keyopt (2) = 2
Wheel frame quality	Mass21	Keyopt (3) = 4
Wheel spring damping	Combin14	Keyopt (2) = 2
Body and suspension connection	Mpc184	Keyopt (1) = 1

2. Contact–Constraint-Based Vehicle–Bridge Coupling Vibration Analysis Method

2.1. Vehicle Model Equivalence Simulation. A vehicle consists of multiple rigid bodies connected by a series or parallel suspension system, and its actual motion is complex. Therefore, researchers simplify the vehicle model to facilitate calculations. The main simplified vehicle models used are the 1/4 vehicle model, 1/2 vehicle model, and full vehicle model.

The 1/2 vehicle model (Figure 1), is always used for the current analysis, because it can reflect the vibration characteristics of the vehicle and is also simpler and more efficient than the whole vehicle model.

Based on the vibration of various components of the vehicle model, the equivalent forms of various types of vehicles in Ansys finite element software are summarized, as shown in Table 1. The beam element can replace the Mpc184 element in the diagram.

2.2. Bridge Model. The bridge model can be built by Ansys finite element software, which should be matched with the vehicle model in the modeling process. For the 1/2 vehicle model, the bridge is used as a beam element model. The more commonly used in vehicle–bridge coupling analysis is Rayleigh damping, calculated as shown in Equation (1):

$$\boldsymbol{C}_b = \alpha \boldsymbol{M} + \beta \boldsymbol{K}, \tag{1}$$

where α and β are the mass damping coefficient and the stiffness damping coefficient, respectively.

2.3. Road Surface Irregularity Simulation. Road surface irregularity is an important excitation in vehicle–bridge coupling vibration and has strong randomness, which must be considered in vehicle–bridge coupling vibration analysis. Currently, in China, road surface irregularity is recorded using power spectral density functions based on measured values. According to the Chinese standard GB/T7031-2005, the expression for road surface power spectrum density can be given as shown in Equation (2):

$$G_q(n) = G_q(n_0)\left|\frac{n}{n_0}\right|^{-w}. \tag{2}$$

In the equation, n and n_0 are the spatial frequency and spatial reference frequency, respectively. Where n_0 is usually taken as 0.1 m^{-1}; $G_q(n_0)$ and $G_q(n)$ are the pavement leveling coefficient and pavement power spectral density function in m^2/m^{-1}, respectively. w is the frequency index, generally taken as 2.

In this study, road surface irregularity is simulated based on the inverse Fourier transform, and the main equations are shown in Equations (3)–(5):

$$|\boldsymbol{X}_k| = \sqrt{\frac{N}{2\Delta L} G_q(n_x)} \quad (k = 0, 1, \ldots\ldots, N/2), \tag{3}$$

$$\boldsymbol{X}(\boldsymbol{k}) = |\boldsymbol{X}_k| e^{i-\varphi_k}, 2\pi \geq \varphi_K \geq 0, \tag{4}$$

$$\boldsymbol{X}_m = \frac{1}{N}\sum_{k=0}^{N-1} \boldsymbol{X}_k e^{\frac{2\pi km}{N} i} \quad (m = 0, 1, \ldots\ldots, N-1). \tag{5}$$

In the above, $|\boldsymbol{X}_k|$ is the modal value of the discrete Fourier transform; n_x, ΔL, N are the spatial frequency sampling points, sampling spacing and number of samples, respectively; $G_q(n_x)$ is the value of the pavement power spectral density function corresponding to the spatial frequency sampling points; and φ_K is the random phase angle on the interval (0, 2π). $\boldsymbol{X}_m$ is the pavement road surface irregularity.

2.4. Ansys-Based Axle Coupling Method. Using Ansys, vehicle model and bridge model can be established, by linking the vehicle and the bridge through the displacement coordination relationship.

It is supposed that the wheels always maintain contact with the bridge when vehicle moves. This can guarantee the vehicle and the bridge satisfy the displacement coordination relationship in Equation (6):

$$Y_{vi} - Y_{bi} = \Delta_i, \tag{6}$$

where Y_{vi} is the vertical displacement of the vehicle wheelbase node; Y_{bi} is the vertical displacement of the bridge at the contact position between the wheelbase node and the bridge; and Δ_i is the sample value of the road surface irregularity at the bottom node of the wheel.

The schematic diagram of the vehicle–bridge coupling calculation model used in this paper is shown in Figure 2.

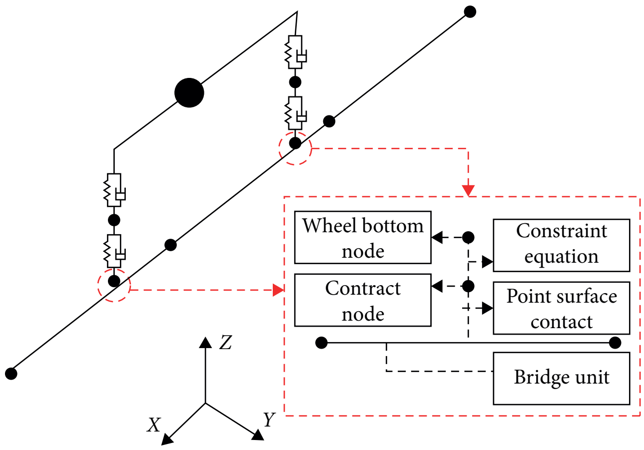

FIGURE 2: Diagram of Ansys vehicle–bridge coupling method based on contact constraint.

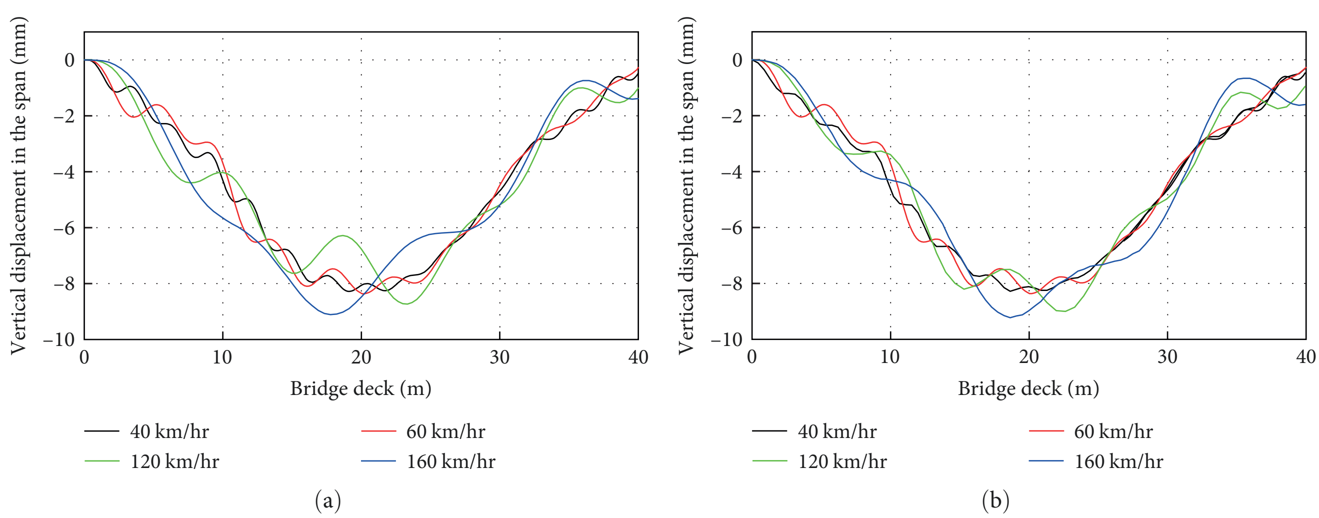

FIGURE 3: Comparison of vertical displacement time history curves: (a) method of this paper and (b) results of literature [24].

Figure 2 represents the implementation of the 1/2 vehicle model. The contact-based analysis method proposed in this paper is entirely based on modeling and solving within the Ansys environment.

2.5. Method Validation. To validate the accuracy of the method proposed in this paper, the vehicle–bridge coupling dynamic model [24] was used for comparison. All parameters were consistent with the values reported in the literature. The calculation model included an 8 m approach bridge, resulting in a total travel length of 40 m. The results of the midspan deflection for the simply supported beam without considering road surface irregularity are shown in Figure 3.

From Figure 3, it shows that the variation pattern of the corresponding time curve in the paper is consistent with that of the literature [24]. When the speed of the vehicle is 40, 60, 120, and 160 km/hr without considering the smoothness of the road surface, the peak vertical displacement response is 8.28, 8.37, 8.73, and 9.11 mm; respectively, calculated by the method of this paper, while the results of the literature [24] are 8.48, 8.48, and 9.11 mm; respectively, 8.51, 8.8, 8.69, and 9.22 mm, the error is less than 2.0%, and the method is more accurate.

3. Vehicle–Bridge Interaction Dynamic Model

3.1. Background. Referring to the main bridge model of Xiaoshaogou Bridge, this bridge is a corrugated steel webs continuous rigid box girder bridge. The main span of the bridge is 57 + 100 + 100 + 57 m. The girder height at the top of the pier is 6.2 m, the girder height at the span middle is 3.2 m, and the girder height is 1.8 parabolic variations of $y_h = 0.00312191 \times 1.8 + 3.2\ \text{m}$ $(45.4\ \text{m} \geq x \geq 0\ \text{m})$. The main girder is made of C55 concrete, the piers are made of C50 concrete, and the corrugated steel webs are made of Q345qD

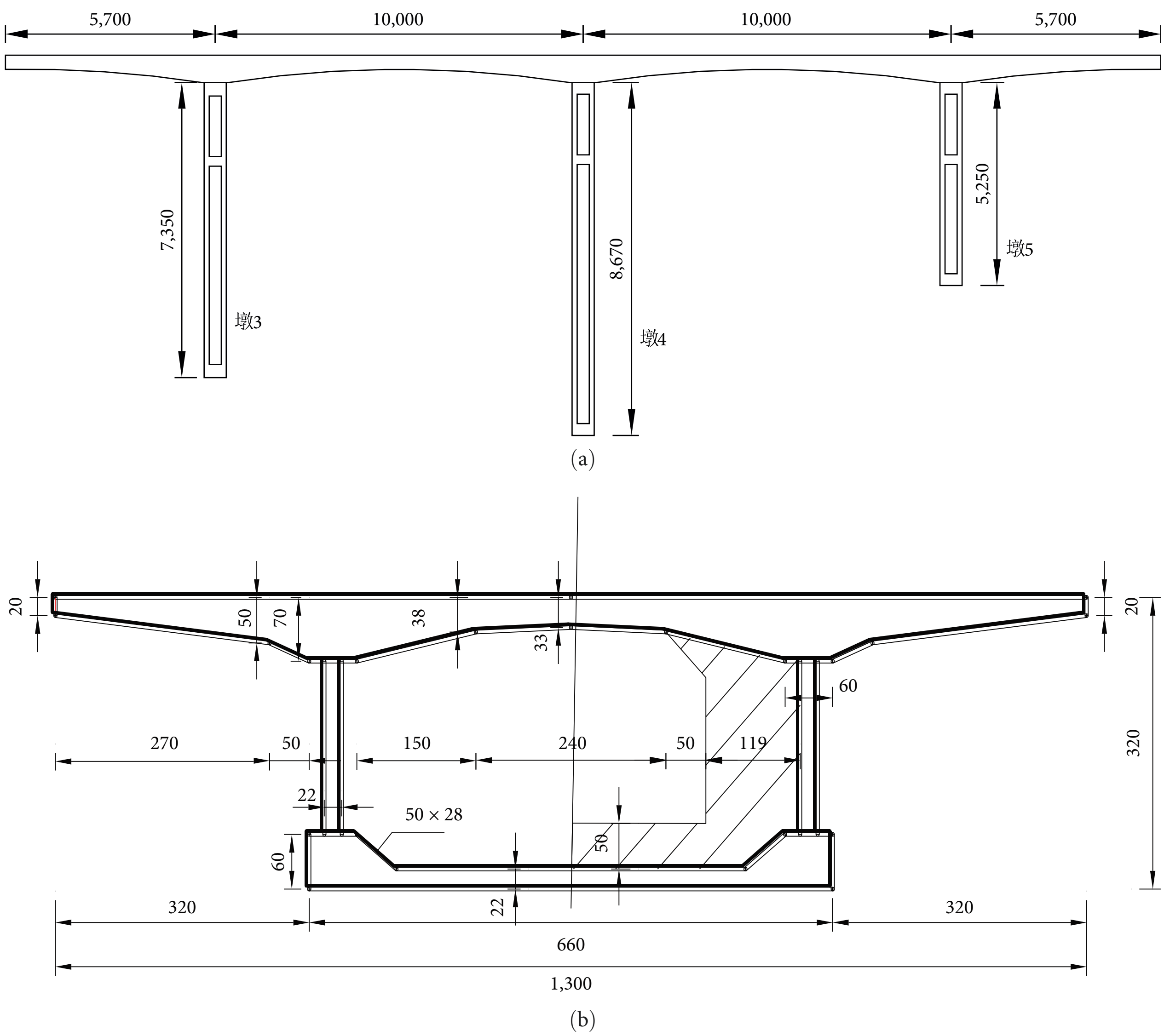

FIGURE 4: Structural diagram of Xiaoshagou bridge: (a) elevation view and (b) cross-sectional dimensions.

steel. The thickness of the steel web is 18–22 mm, wavelength 1.6 m, and wave height 0.22 m. The main pier adopts rectangular hollow section, which is 6 × 6.6 m. The height of the three main piers from left to right is 73.5, 86.7, and 52.5 m. The schematic diagram of the structure of Xiaoshagou Bridge is shown in Figure 4.

3.2. Vehicle Models. The 1/2 vehicle model provides more accurate results compared to the full vehicle model, and its computational speed is faster. Based on reference [25], the 1/2 two-axle vehicle model used in this paper was selected. Four degrees of freedom were considered in the analysis: vertical bounce, pitch, and vertical bounce between the vehicle body and the wheelset. The vehicle diagram and specific parameters are shown in Figure 5 and Table 2.

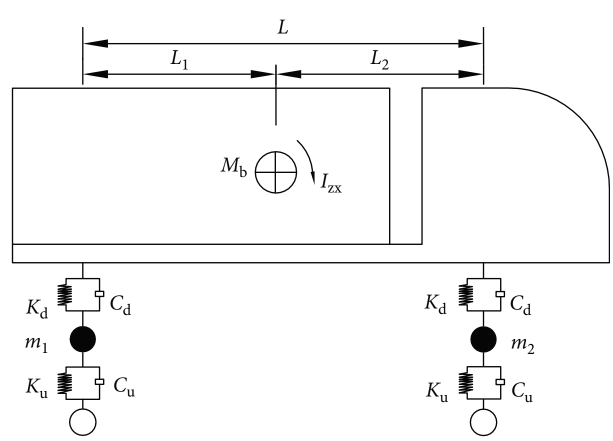

FIGURE 5: Diagram of vehicle model diagram.

Table 2: Parameters of 1/2 vehicle model.

Parameter	Symbol	Unit	Value
Gross vehicle weight	GVW	t	36.532
Body mass	M_b	t	28.054
Pitch rotation inertia	I_{zx}	kg.m^2	172,160
Suspension and wheels quantity	m_1 and m_2	t	4.239
One series of spring rigid degree	K_u	kN/m	2,000
One series of damping system	C_u	kN·s/m	10
Number second series spring rigid	K_d	kN/m	1,903.172
Second system damping system number	C_d	kN·s/m	40
Front axle-body center of mass distance	L_1	m	4.2
Rear axle-body distance from the center of mass	L_2	m	4.2
Total vehicle length	L	m	8.4

Table 3: First six natural frequencies and modes of the Xiaoshagou bridge.

Model state	Frequency (Hz)	Period (s)	Vibration mode
1	0.49890	2.0044	First-order transverse bend
2	0.64844	1.5421	First-order side-shift
3	1.0459	0.9561	Second-order antisymmetric transverse bends
4	1.4676	0.6814	Third-order horizontal bend
5	1.5457	0.6470	First-order antisymmetric vertical bend
6	1.9735	0.5067	Second-order symmetric vertical bend

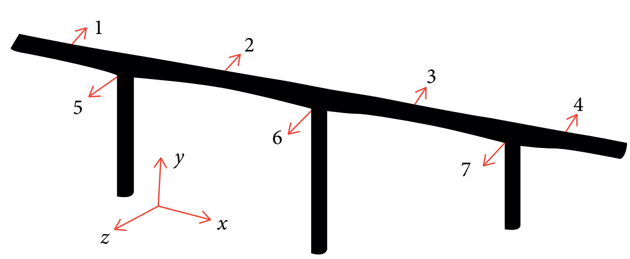

Figure 6: Control section and FEA model of Xiaoshagou bridge.

3.3. Bridge Finite Element Model. The bridge is modeled in Ansys by Beam189, which totally consists of 325 elements and 979 nodes.

The modal analysis of the main structure of the Xiaoshaogou Bridge is performed by using the Ritz vector method. The free vibration frequencies of the first six modes are shown in Table 3, The control section 1–7 (middle span and pier top of each span) and finite element model are shown in Figure 6.

To verify the proposed bridge model, the free vibration frequencies and vibration modes were compared with those of the literature [26]. The bridge-pier-pile model developed in the literature [26] has first-order transverse bending and first-order antisymmetric vertical bending frequencies of 0.452287 and 1.453605 Hz, respectively, which are slightly smaller than the results of this paper. The flexibility of the bridge will be slightly increased and the free vibration frequency will be reduced after considering the influence of piles. The correctness of the bridge model in this paper can be verified.

4. Vehicle–Bridge Coupled Response under Seismic Excitation

Based on the proposed vehicle–bridge coupling method, the direct input of seismic acceleration records was used. According to the "Specifications for Seismic Design of Highway Bridges" (JTG/T 2231-01-2020) [27], assuming that the ground motion is consistent at all support locations of the bridge and considering that the continuous rigid frame bridge does not exceed 600 m, the effect of wave propagation can be neglected. The integration time step and seismic acceleration records were set to 0.02 s.

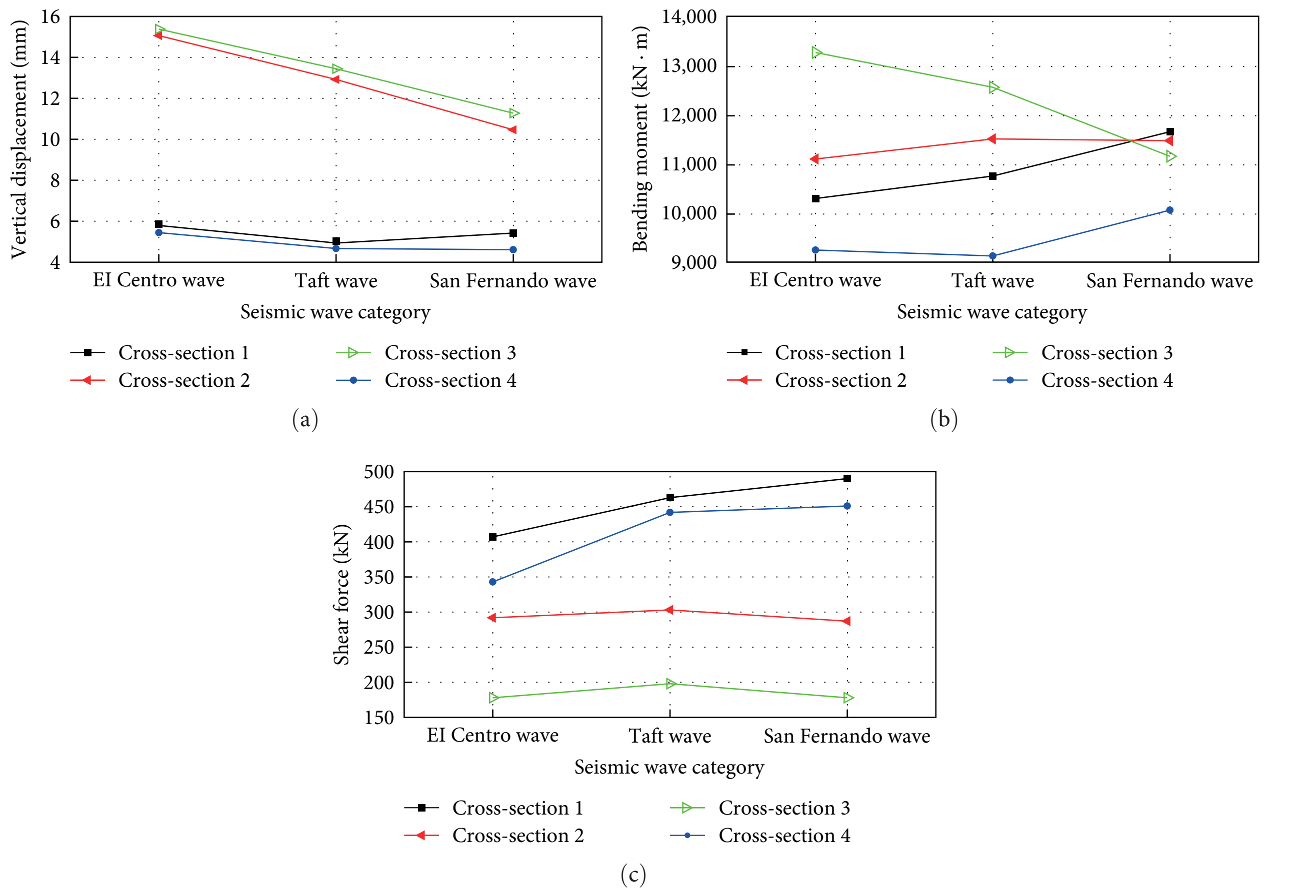

FIGURE 7: Maximum dynamic response of bridge girder under different seismic wave: (a) vertical displacement, (b) bending moment, and (c) shear force.

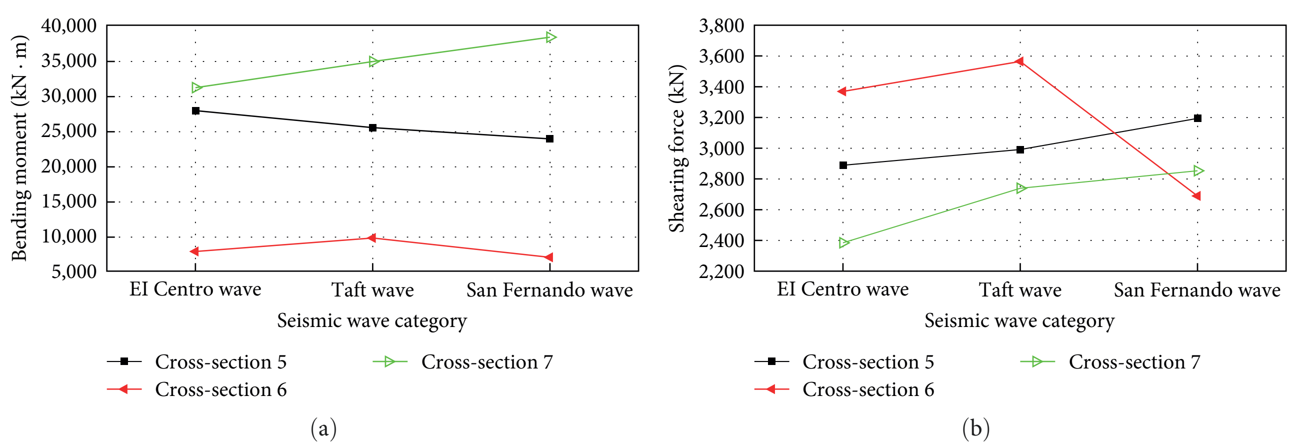

FIGURE 8: Maximum dynamic response of bridge piers under different seismic wave: (a) bending moment and (b) shear force.

4.1. Effects of Seismic Wave Types. Keeping the vehicle speed at 60 km/hr, the EI Centro wave, Taft wave, and San Fernando wave were respectively modified to have an acceleration amplitude of 0.1 g and used to analyze the seismic-vehicle-bridge coupling responses for different seismic wave types.

Figures 7 and 8 show the maximum dynamic responses of the bridge girder and the bridge pier for the three types of seismic wave inputs. From Figures 7 and 8, the peak displacement dynamic responses of EI Centro, Taft, and San Fernando waves are 5.794, 4.937, and 5.422 mm, respectively, at Section 1; the peak bending moment responses are 10295×10^6, 10750×10^6, and $11{,}652 \times 10^6$ kN·m, respectively. The peak shear response was 407, 463, and 490 kN. The peak displacement at Section 1 changes by 17.3%, the peak bending moment changes by 13.2%,

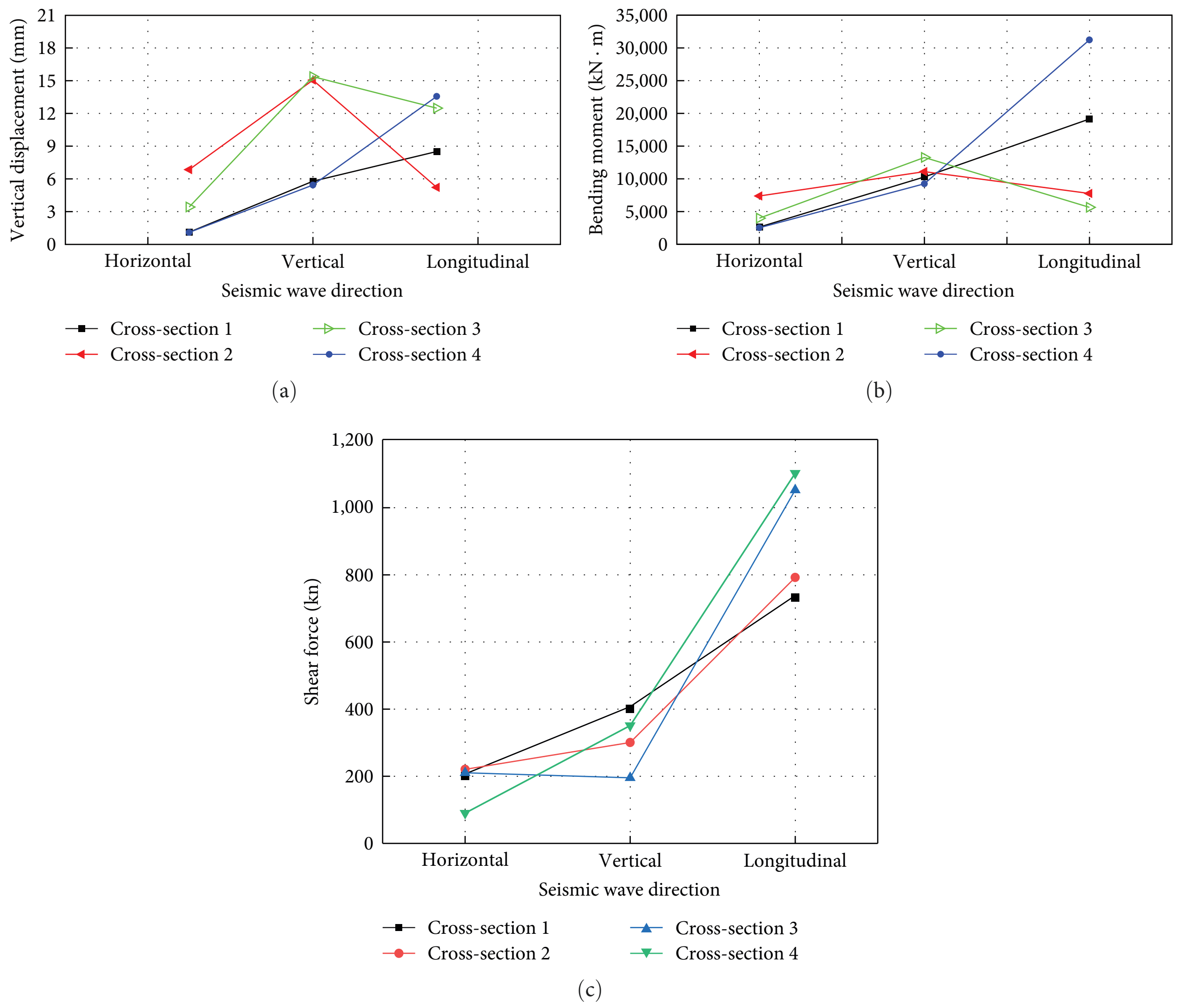

FIGURE 9: Maximum dynamic response of bridge deck in different seismic wave directions: (a) vertical displacement, (b) bending moment, and (c) shear force.

and the peak shear force changes by 20.4%. The peak of each response does not correspond to the same seismic wave, and the peak displacement, bending moment, and shear dynamic response of the section does not correspond to the same seismic wave. It is suggested that all the displacement, bending moment, and shear response under different seismic waves should be considered respectively.

Combining the results of the seven different control sections, the maximum difference of 31.4% for the bridge girder and 39.5% for the bridge pier after considering different types of seismic waves. The main reason is that the coupled seismic vehicle–bridge response is not only affected by the peak seismic. It should also be related to the spectral characteristics of the ground vibration, and the cross-section at the location of the bridge pier is also the same law.

4.2. Seismic Wave Direction Effects. Keeping the vehicle speed at 60 km/hr and other factors constant, the EI Centro waves of 0.1 g were input in the transverse, vertical, and longitudinal directions as shown in Figure 7(a), and the coupled seismic-vehicle-bridge analysis was performed respectively. The maximum dynamic response of the bridge girder and the top of the bridge pier are shown in Figures 9 and 10.

From Figures 9 and 10, it shows that the vertical response of the bridge under transverse ground shaking is much less than that of vertical and longitudinal ground shaking in most cases, while the longitudinal ground shaking has the greatest effect on the moment response of the bridge piers and the vertical ground shaking has the greatest effect on the shear force of the bridge piers and the effect on the displacement of the bridge deck cannot be ignored. For the bridge girder, the ratio of the bridge response under vertical or longitudinal Seismic excitation to the response of transverse seismic excitation is 1.50–12.31; for the bridge pier, the ratio is 2.48–26.61. The result imply that the effect of vertical and longitudinal seismic excitation must be considered when analyzing the vertical dynamic response of the earthquake-vehicle-bridge coupling.

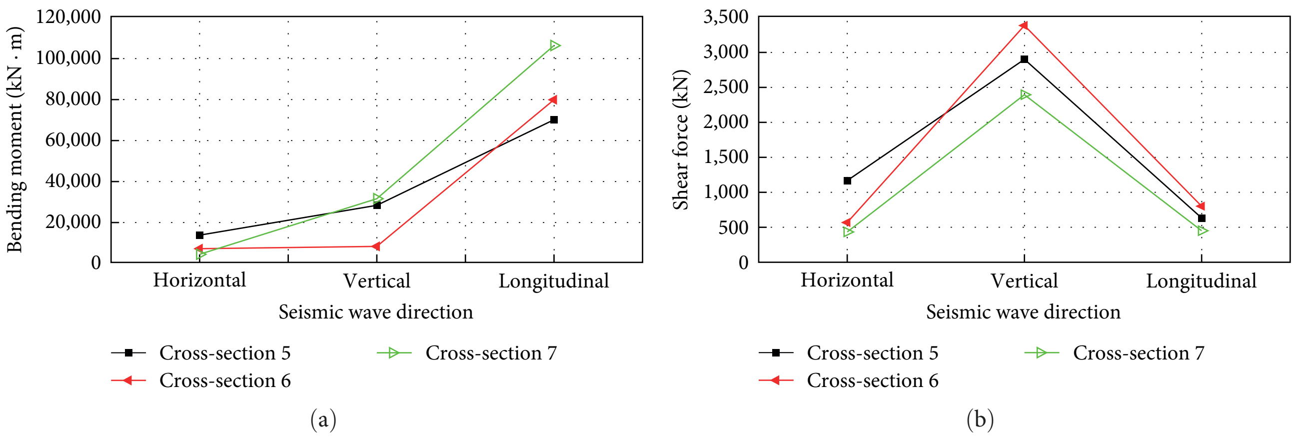

FIGURE 10: Maximum dynamic response of bridge piers in different seismic wave directions: (a) bending moment and (b) shear force.

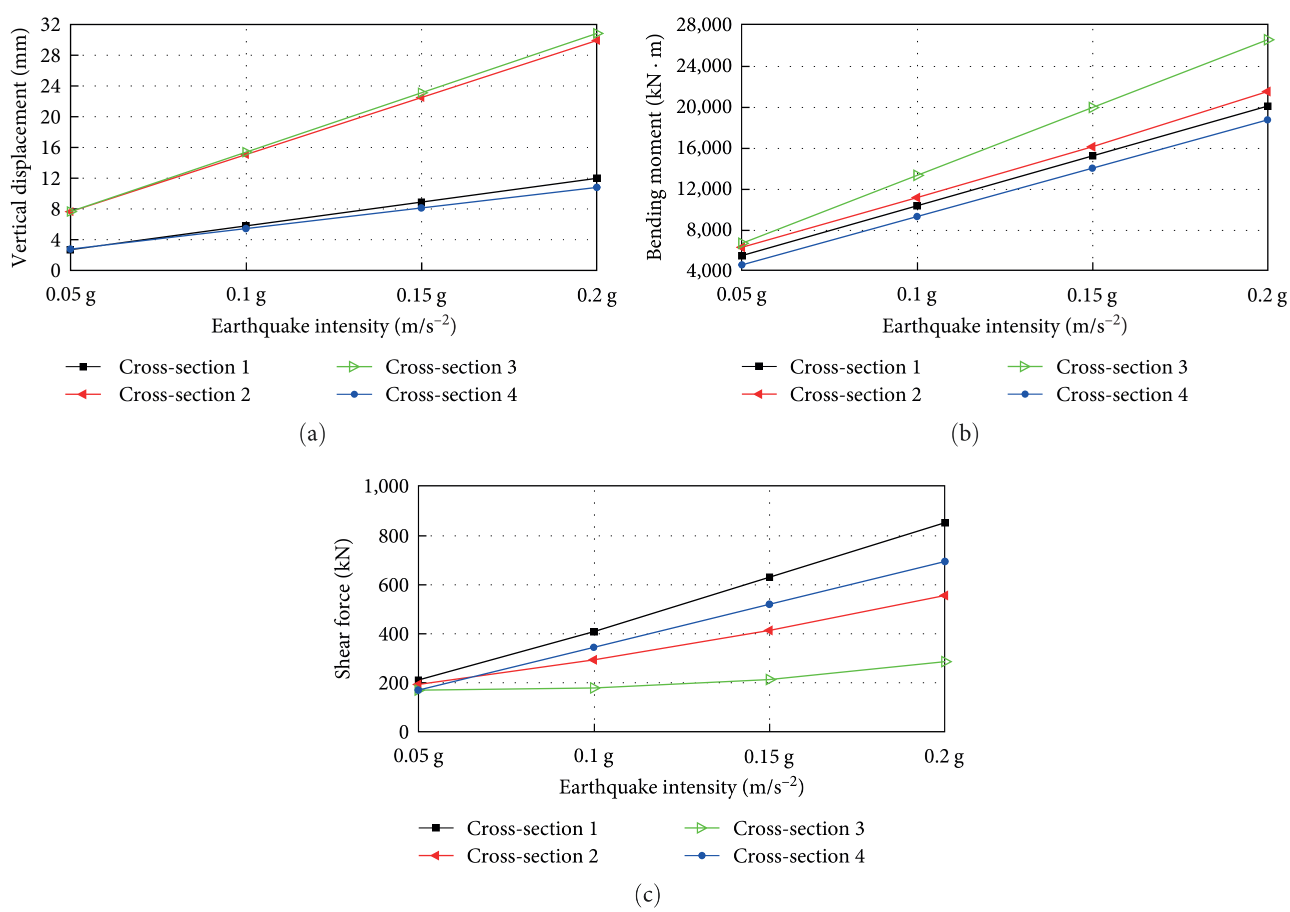

FIGURE 11: Maximum dynamic response of bridge decks of different seismic wave categories: (a) vertical displacement, (b) bending moment, and (c) shear force.

4.3. Seismic Wave Intensity Effects. Keeping the vehicle speed at 60 km/hr and other factors constant, the EI Centro wave was input along the vertical direction, and its amplitude was adjusted to 0.05, 0.1, 0.15, and 0.2 g to study the coupled seismic-vehicle-bridge vibration for different seismic wave intensity pairs. The maximum dynamic response of the bridge deck and the top of the bridge pier are shown in Figures 11 and 12.

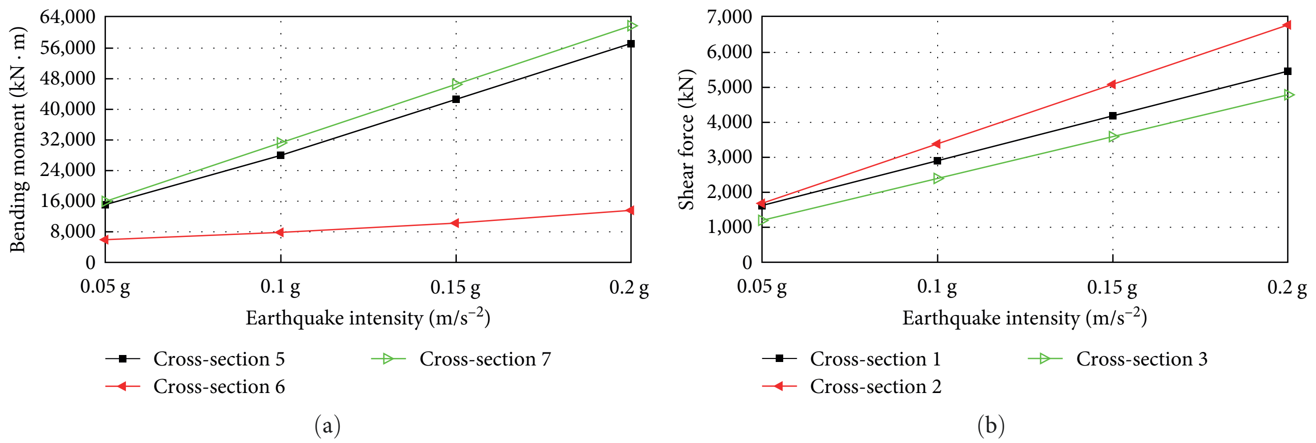

Figure 12: Maximum dynamic response of bridge piers with different seismic wave categories: (a) vertical displacement and (b) bending moment.

From Figures 11 and 12, it can be seen that the dynamic response of the beam increases approximately in proportion to the increase in the seismic intensity level. Taking Section 1 as an example, the calculated displacements under seismic waves at 0.05, 0.1, 0.15, and 0.2 g are 2.702, 5.794, 8.889, and 11.985 mm, respectively, with a displacement ratio of 1 : 2.14 : 3.289 : 4.435; the calculated bending moment values are 5,437, 10,295, 15,154, and 20,016 kN·m with bending moment ratio of 1 : 1.894 : 2.787 : 3.681; the calculated shear values are: 210, 407, 628, and 850 kN, the ratio is 1 : 1.938 : 2.99 : 4.048. The response at cross-section of the bridge pier is also by this law. The displacement, bending moment, and shear force are not kept exactly same proportional because of other factors such as bridge self-weight, vehicle system, and damping of the coupled system. For general cases, it can be approximated that the ground vibration intensity is proportional to the response value.

5. Simplification of Seismic-Vehicle-Bridge Coupling Vibration

In this section, based on the research results from Section 4.2, only vertical and longitudinal seismic waves were input to analyze the seismic-vehicle-bridge coupling vibrations.

5.1. Effects of Vehicle Speed. Keeping other parameters constant, the EI Centro seismic wave with an amplitude of 0.1 g was input in the longitudinal and vertical directions. The dynamic responses of the bridge were studied under vehicle speeds of 60, 90, and 120 km/hr, with the same duration of seismic motion of 18.84 s. The maximum dynamic responses on the bridge girder and pier tops are shown in Figures 13 and 14.

From Figures 13 and 14, it can be obtained that the displacement, bending moment, and shear force responses of the bridge are slightly different under different vehicle speeds, but the peak values of the dynamic responses are not significantly affected. The dynamic responses of the control sections are generally consistent. Take Section 1 as an example, when the vehicle is traveling at 60, 90, and 120 km/hr, the peak displacement of the bridge is 9.256, 9.145, and 9.246 mm, the peak bending moment is 20,075, 20,388, and 19,856 kN·m, and the peak shear force is 858 and 853 kN. The peak shear forces are: 858, 853, and 844 kN, the difference between the maximum and minimum value is about 1.2%. The effect of vehicle speed is less than 7.2%, and the effect of vehicle speed can be ignored to simplify the calculation.

5.2. Effects of Road Surface Irregularity Randomness. Road surface irregularity exhibits strong randomness, and many domestic and foreign researchers have conducted extensive studies on the randomness of vehicle–bridge coupling vibration [28]. To study the impact of road surface irregularity randomness on the seismic-vehicle-bridge coupling vibration, a vehicle speed of 60 km/hr was maintained, and three different road surface irregularity sequences of the same grade were selected. The maximum dynamic responses on the bridge deck and pier tops are shown in Figures 15 and 16.

From Figures 15 and 16, it can be obtained that for different pavements of the same road surface irregularity, the peak values of displacement, bending moment, and shear response of road surface irregularity sequence for the coupled seismic-vehicle-bridge vibration are almost the same, and the overall difference is within 3% without considering the effect of the randomness of pavement unevenness. Therefore, it is concluded that the randomness of road surface irregularity can be neglected in the seismic-vehicle-bridge coupled vibration.

5.3. Effects of Road Surface Irregularity Grade. With a seismic excitation speed of 60 km/hr and other parameters constant, three different grades of road surface irregularity sequences (A, B, and C) were selected to study the effects of different road surface irregularity grades on the seismic-vehicle-bridge coupling vibration. A comparison was also made with the seismic bridge response and the vehicle-bridge coupling response (considering road surface irregularity Grade D). The maximum dynamic responses on the bridge deck and pier tops are shown in Figures 17 and 18. In the figures, G1, G2, G3, G4, G5, and G6 represent the seismic-vehicle-bridge coupling responses with road roughness grades A, B, C, and D, the seismic bridge vibration response without considering

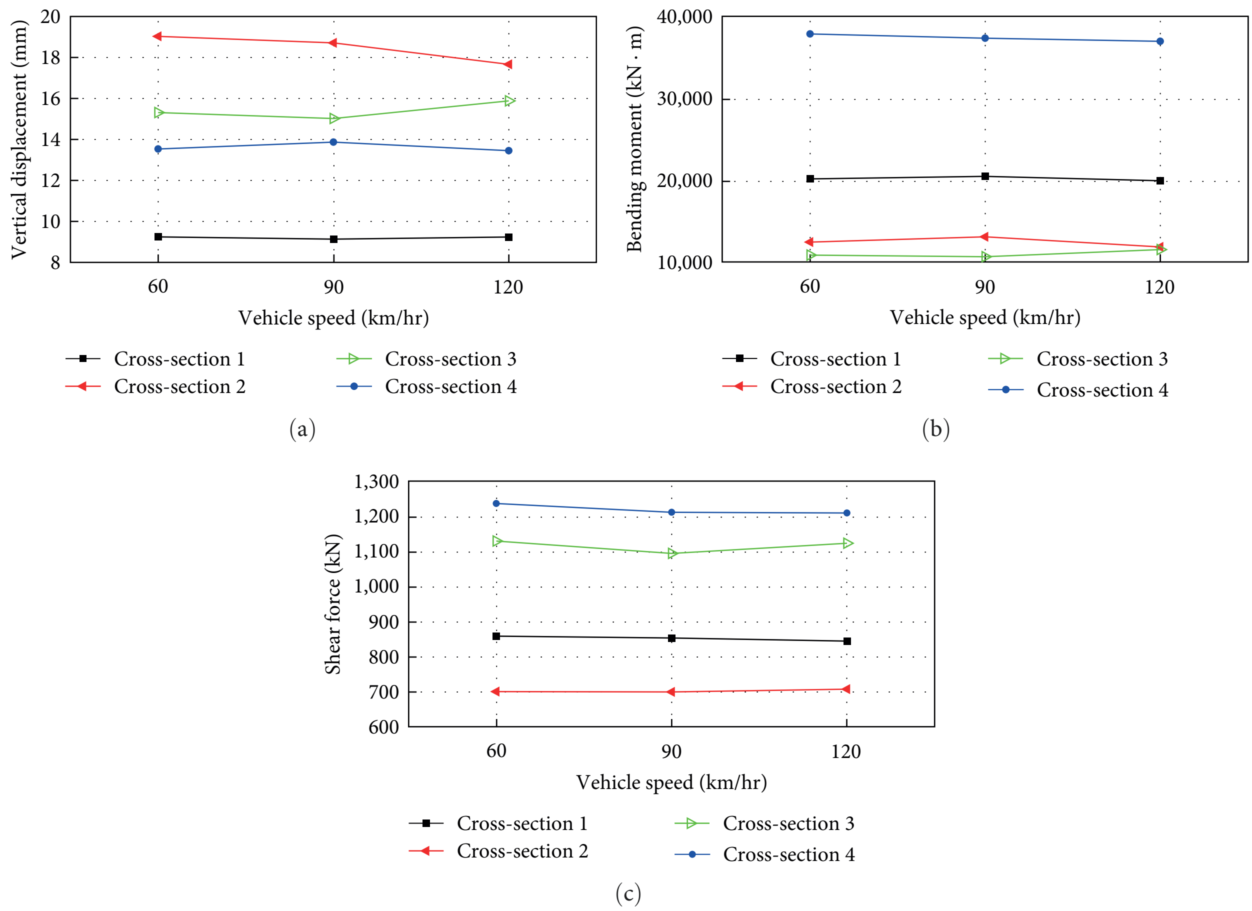

Figure 13: Maximum dynamic response of bridge girder at different vehicle speeds: (a) vertical displacement, (b) bending moment, and (c) shear force.

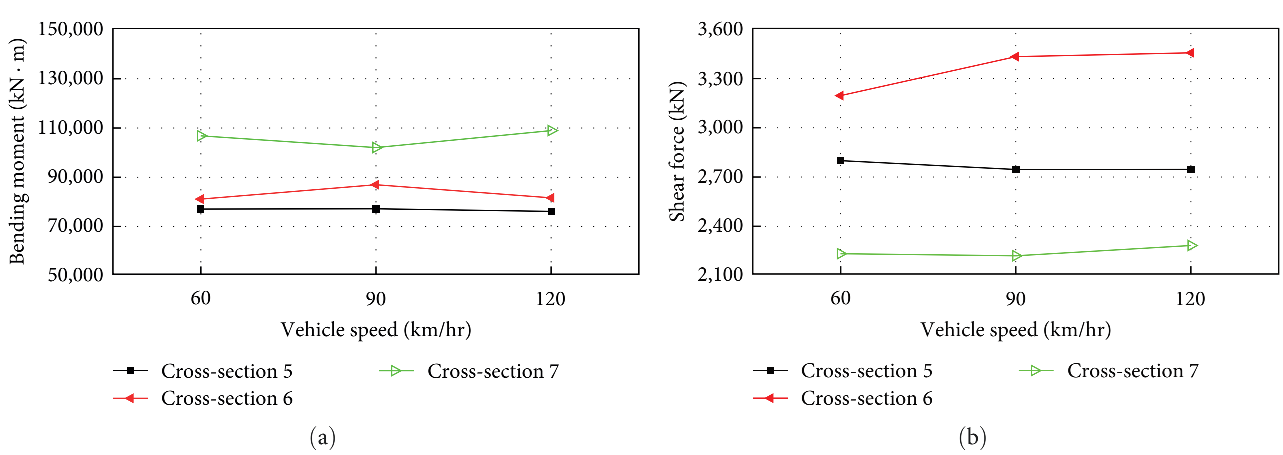

Figure 14: Maximum dynamic response of bridge piers at different vehicle speeds: (a) vertical displacement and (b) bending moment.

road roughness, and the response without seismic-vehicle-bridge coupling.

From Figures 17 and 18, it can be obtained that the peak displacement of the bridge at Section 1 under the six conditions mentioned in the paper are: 9.255, 9.253, 9.266, 9.309, 9.256, and 1.452 mm, the peak bending moment are: 20,074, 20,004, 20,003, 19,883, and 3,571 kN·m, and the peak shear force are: 858, 857, 858, 857, 858, 344, 20,075, and 3,571 kN·m; the peak shear forces are: 858, 857, 858, 857, 858, and 344 kN, and similar results for other sections. Without seismic excitation, the peak dynamic response is significantly smaller compared to the coupled seismic-vehicle-bridge

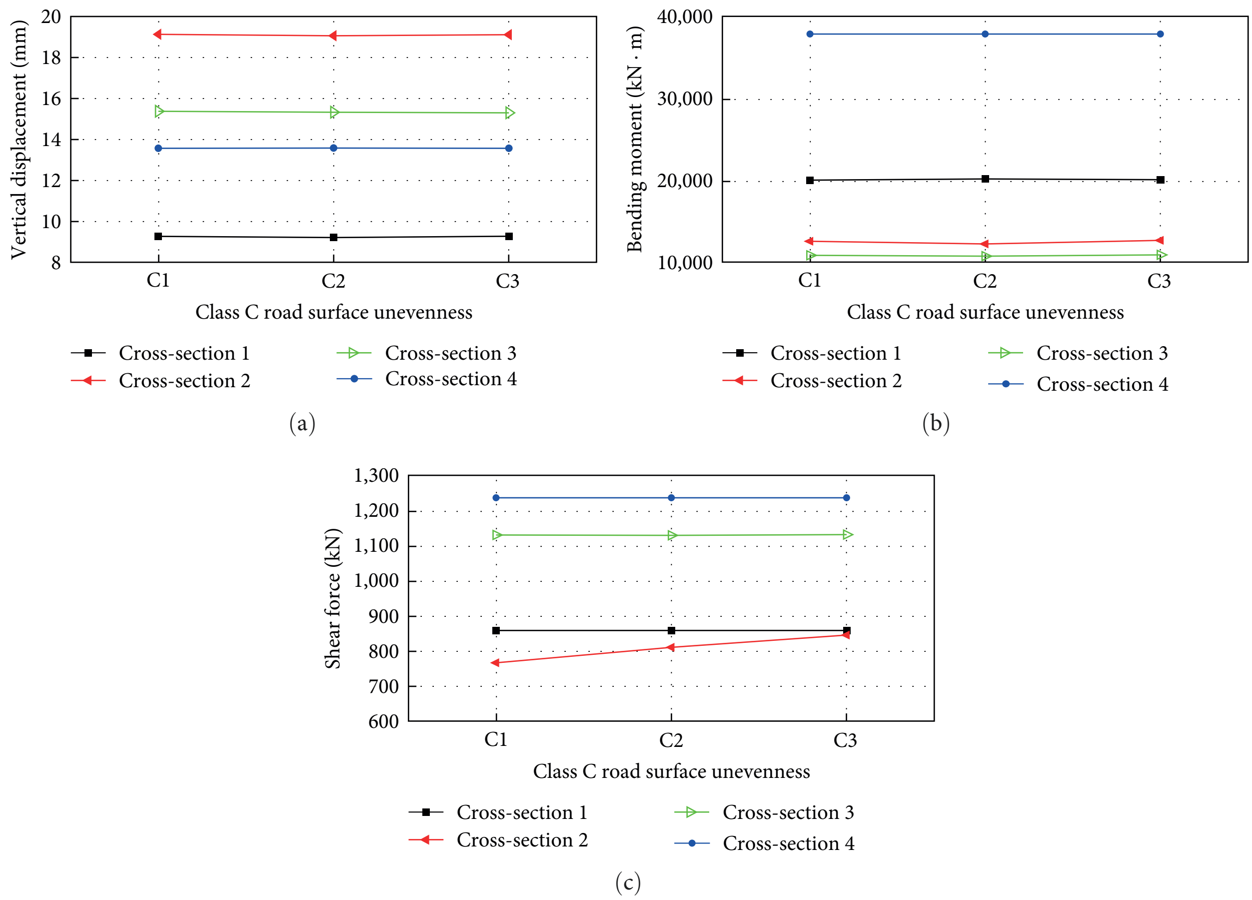

Figure 15: The maximum dynamic response of bridge girder with different road surface irregularity: (a) vertical displacement, (b) bending moment, and (c) shear force.

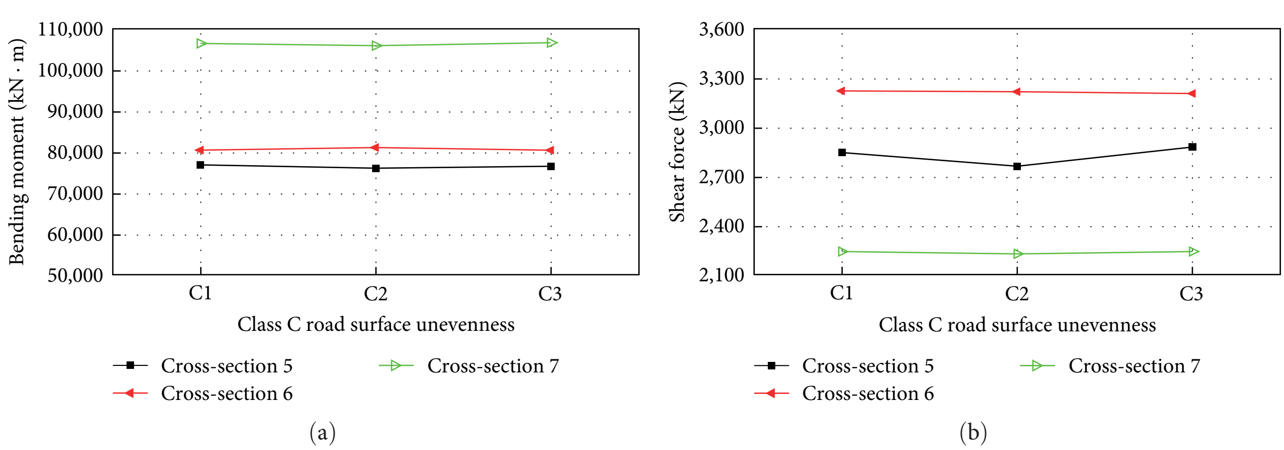

Figure 16: The maximum dynamic response of bridge piers with different road surface irregularity: (a) vertical displacement and (b) bending moment.

response, while the seismic bridge response is consistent with the coupled seismic-vehicle-bridge response, mainly because the vehicle load is smaller compared to the self-weight of the bridge. Another reason is that because for each midspan section, the time of the peak vibration response of the coupled vehicle–bridge response is different from the time of the peak seismic bridge response. Therefore, the dynamic response problem of seismic-vehicle-bridge-coupling can be simplified to the seismic-bridge vibration problem. The difference in the dynamic response of the bridge under each level of road

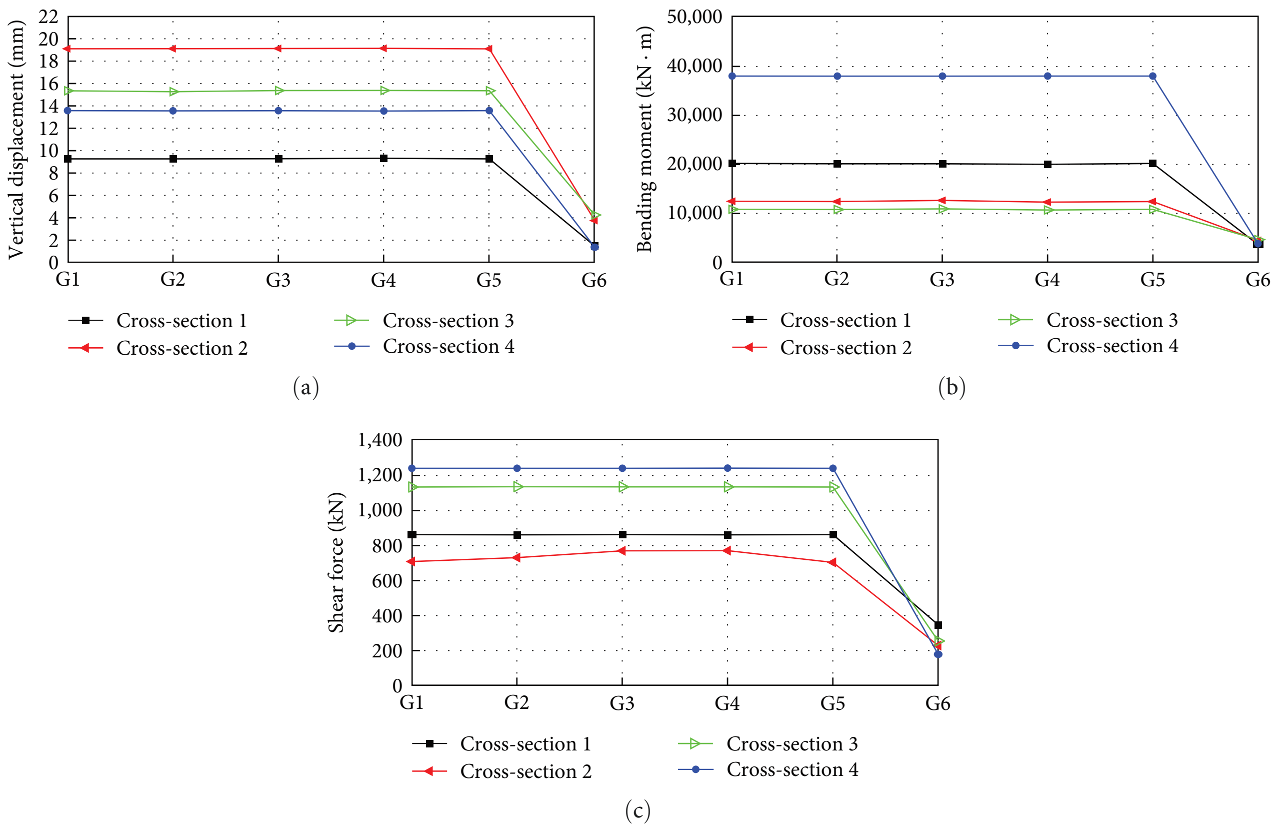

FIGURE 17: Maximum dynamic response of bridge decks with a different grad of road irregularity: (a) vertical displacement, (b) bending moment, and (c) shear force.

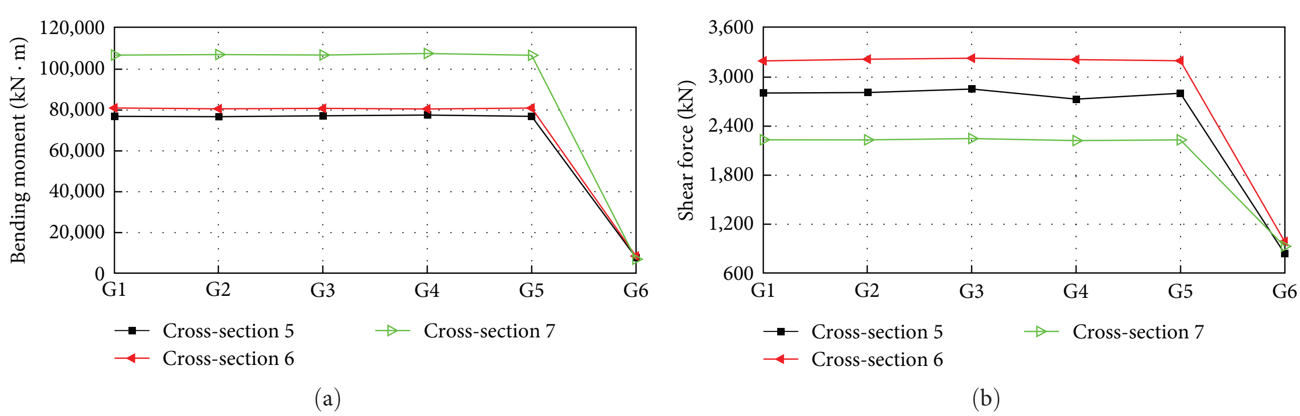

FIGURE 18: Maximum dynamic response of bridge piers with a different grad of road irregularity: (a) vertical displacement and (b) bending moment.

surface irregularity not exceed 1%, the effect of road surface irregularity level can be ignored when performing seismic-vehicle-bridge coupling.

6. Conclusion

In this study, a contact-constrained vehicle–bridge coupling vibration analysis method was proposed, and a seismic-vehicle-bridge coupling vibration model was established to analyze the dynamic response of bridges under seismic loads. The effects of seismic wave categories, directions, and intensities on the bridge's dynamic response were investigated. Furthermore, the effects of vehicle speed, road surface irregularity grade, and randomness in the seismic-vehicle-bridge coupling were studied by inputting vertical and longitudinal seismic motions. A comparison was made between the seismic bridge vibration, seismic-vehicle-bridge coupling vibration, and vehicle–bridge coupling vibration responses. The following conclusions can be drawn:

(1) The vehicle model was simplified by introducing contact nodes and establishing contact equations with the bridge and constraint equations with the vehicle. Compared to existing methods, this approach is more efficient and ensures a higher level of accuracy in considering the effects of road surface irregularity on seismic-vehicle-bridge coupling vibration.

(2) Seismic wave directions have a different impact on dynamic response of the bridge. When studying the vertical vibration of the bridge, it is necessary to consider vertical and longitudinal seismic excitation. Furthermore, a comprehensive analysis including displacement, bending moment, and shear force dynamic responses should be conducted.

(3) The ground shaking intensity is basically approximately proportional to the dynamic response of the bridge. The dynamic response of the coupled seismic–vehicle bridge is not only related to the seismic intensity but also the seismic category.

(4) After considering seismic loads, the influence of vehicle speed and road surface irregularity is generally less than 3% on the structure response and can be neglected. The randomness of road surface irregularity can also be neglected, too. In practical engineering, for simplicity, the analysis of bridge response under seismic-vehicle-bridge coupling can directly focus on the bridge's response under seismic action.

(5) This study did not consider the motion of seismic waves at different supports and did not analyze the dynamic response of vehicle sequence, multilane vehicles under seismic conditions for continuous rigid frame box girder bridge with corrugated steel webs. Further research may be carried out on these aspects in the future.

Data Availability

The (1/2 vehicle model provides more accurate results) data used to support the findings of this study are available from the corresponding author upon request.

Conflicts of Interest

The authors declare that they have no conflicts of interest.

Acknowledgments

This work is financially supported by the National Natural Science Foundation of China Major Project (52192663): Multi-dimensional Characterization Indicators of Structural Service Performance and Its Intelligent Evaluation Theory and Methods and the Shaanxi Provincial Natural Science Basic Research Program Project (2021JM-181): Research on Assessment Methods of Technical Condition and Carrying Capacity of Existing Bridges Based on Big Data Analysis.

References

[1] P. Qiao, C.-X. Zhong, Z.-Y. Wang, and A.-Y. Wang, "State-of-the-art and trend of studies on vehicle–bridge coupling vibration in China," *Journal of Chong Qing Jiao Tong University: Natural Science*, vol. 38, no. 12, pp. 26–37, 2019.

[2] L. Xiang, L.-Z. Jiang, P. Xiang, J.-F. Mao, and M.-L. Wei, "Analysis of train–bridge vertical random vibration based on a new point estimate method," *Journal of Vibration and Shock*, vol. 39, no. 6, pp. 15–21, 2020.

[3] Z.-X. Li, J. Huang, Y. Zhang, and G.-Z. Zhang, "Influence of seismic excitation on coupled vibration of train-bridge system in light railway," *Earthquake Engineering and Engineering Vibration*, vol. 25, no. 6, pp. 183–188, 2005.

[4] Z. Li, E.-D. Guo, Q. He, and S.-J. Liang, "Dynamic responses and train running safety of railway cable-stayed bridge under earthquake," *Engineering Mechanics*, vol. 34, no. 4, pp. 78–87 +100, 2017.

[5] L. Hujun, L. Xiaozhen, and L. Dejun, "Train running safety analysis of high-pier rigid frame bridge under earthquake action," *Earthquake Engineering and Engineering Vibration*, vol. 34, no. 5, pp. 87–93, 2014.

[6] X. Du, X. He, and Y. Zhu, "Research on ground motion input mode in vehicle–bridge coupling dynamic analysis," *China Railway Science*, vol. 32, no. 6, pp. 34–40, 2011.

[7] L. Hujun and L. Xiaozhen, "Input methods of non-uniform seismic excitation in coupling system of vehicle-track-bridge," *Journal of Railway Science and Engineering*, vol. 12, no. 4, pp. 769–777, 2015.

[8] L. Zhi, G. Endong, and H. Qian, "Seismic response analysis of train-bridge coupling system on high-speed railway," *Earthquake Engineering and Engineering Vibration*, vol. 35, no. 3, pp. 119–124, 2015.

[9] D. Ziming, G. Xiangrong, and Z. Zhiyong, "Coupled vibration of train-bridge system of steel truss bridge with seismic effect," *Journal of Central South University: Science and Technology*, vol. 32, no. 1, pp. 184–191, 2011.

[10] Y. Chengzhao, *Analysis and Research on Coupled Vibration of Highway Vehicle Bridge Considering the Influence of Deck Irregularity*, Central South University, Changsha, 2011.

[11] T. Wang, W. S. Han, F. Yang, and W. Kong, "Wind-vehicle–bridge coupled vibration analysis based on random traffic flow simulation," *Journal of Traffic and Transportation Engineering*, vol. 1, no. 4, pp. 293–308, 2014.

[12] Y. Li, C. S. Cai, Y. Liu, Y. Chen, and J. Liu, "Dynamic analysis of a large span specially shaped hybrid girder bridge with concrete-filled steel tube arches," *Engineering Structures*, vol. 106, pp. 243–260, 2016.

[13] Y. Jianrong, *Local Dynamic Response of Highway Bridges to Moving Vehicles*, Tongji University, Shanghai, 2007.

[14] Y. Jianrong, *Research on Vehicle–Bridge Coupling Vibration of Continuous Rigid Frame Bridge with Composite Box Girder with Corrugated Steel Webs*, Lanzhou Jiaotong University, Lanzhou, 2017.

[15] I. Peiwen, H. Shuanhai, and S. Yifan, "Vehicle–bridge coupled vibration and its influencing factors of simple beam," *Journal of Chang'an University: Natural Science Edition*, vol. 33, no. 1, pp. 59–65, 2013.

[16] L. Shizhong, *Research on Vehicle–Bridge Coupled Vibration of Double-Deck Highway Steel Truss Bridge*, Chang'an University, Xian, 2015.

[17] C. Xiaodong, *The Vehicle–Bridge Interaction Analysis of Corrugated Steel Web Box Girder Based on Contact-Constraint Method*, Chongqing University, Chongqing, 2019.

[18] Z. Jin, S. Pei, X. Li, H. Liu, and S. Qiang, "Effect of vertical ground motion on earthquake-induced derailment of railway vehicles over simply-supported bridges," *Journal of Sound and Vibration*, vol. 383, pp. 277–294, 2016.

[19] T. S. Paraskeva, E. G. Dimitrakopoulos, and Q. Zeng, "Dynamic vehicle–bridge interaction under simultaneous vertical earthquake excitation," *Bulletin of Earthquake Engineering*, vol. 15, no. 1, pp. 71–95, 2017.

[20] J. Zhou, C. Huang, J. Deng, J. Zhang, and L. Zhang, "A co-simulation approach for straddle monorail vehicle–bridge interaction subjected to nonlinear excitation," *Advances in Engineering Software*, vol. 180, Article ID 103458, 2023.

[21] J. Su, J. Zhang, J. Zhou, C. Hu, and Y. Zheng, "Fatigue life assessment of suspenders in tied-arch bridges under random traffic loads and environmental corrosion," *International Journal of Civil Engineering*, vol. 21, no. 3, pp. 523–540, 2023.

[22] H. Yu, B. Wang, Y. Li, Y. Zhang, and W. Zhang, "Road vehicle–bridge interaction considering varied vehicle speed based on convenient combination of Simulink and ANSYS," *Shock and Vibration*, vol. 2018, Article ID 1389628, 14 pages, 2018.

[23] Q. Zou, L. Deng, T. Guo, and X. Yin, "Comparative study of different numerical models for vehicle–bridge interaction analysis," *International Journal of Structural Stability and Dynamics*, vol. 16, no. 9, Article ID 1550057, 2016.

[24] C. Xiaodong, *Vehicle–Bridge Coupled Dynamical Numerical Analysis Based on ANSYS for Large Span Continuous Rigid Frame Bridge with High Piers*, Chang'an University, Xi'an, 2019.

[25] L. Deng, L.-L. Duan, W. He, and W. Yi, "Study on vehicle model for vehicle–bridge coupling vibration of highway bridges in China," *China Journal of Highway and Transport*, vol. 31, no. 7, pp. 92–100, 2018.

[26] L. Ming, *Static and Dynamic Characteristics Analysis and Seismic Study of PC Continuous Rigid Frame Bridge with Corrugated Steel Webs*, Lanzhou Jiaotong University, Lanzhou, 2017.

[27] JTG/T2231-01-2020, *Specifications for Seismic Design of Highway Bridges*, China Communication Press, Beijing, 2020.

[28] L. Deng and C. S. Cai, "Identification of parameters of vehicles moving on bridges," *Engineering Structures*, vol. 31, no. 10, pp. 2474–2485, 2009.